Science
AAAS

Control Profiles of Complex Networks

Justin Ruths and Derek Ruths

Science **343**, 1373 (2014);
DOI: 10.1126/science.1242063

Science (print ISSN 0036-8075; online ISSN 1095-9203) is published weekly, except the last week in December, by the American Association for the Advancement of Science, 1200 New York Avenue NW, Washington, DC 20005.

Control Profiles of Complex Networks

Justin Ruths[1]* and Derek Ruths[2]

Studying the control properties of complex networks provides insight into how designers and engineers can influence these systems to achieve a desired behavior. Topology of a network has been shown to strongly correlate with certain control properties; here we uncover the fundamental structures that explain the basis of this correlation. We develop the control profile, a statistic that quantifies the different proportions of control-inducing structures present in a network. We find that standard random network models do not reproduce the kinds of control profiles that are observed in real-world networks. The profiles of real networks form three well-defined clusters that provide insight into the high-level organization and function of complex systems.

Many natural complex systems are important or vital to human life, society, and governance. Undesirable behavior of such systems, observed in the form of disease, epidemics, economic collapse, and social unrest, has generated considerable interest in being able to control complex systems modeled as networks. Previous work has already established the connection between control theory and complex networks (*1*–*3*). Controlling a complex directed network reduces to (i) the selection of specific nodes that, by virtue of being directly controlled, can indirectly drive the rest of the network to any arbitrary state and (ii) the prescription of time-varying control inputs that, when applied to these nodes, will drive the system to a desired state.

Work to date has focused on the number of controls and their attachment points required by a complex network (*4*). Existing studies have shown how the mathematics of structural controllability can be used to identify a minimum number of controls that can drive the system as a whole to any arbitrary state. A main outcome of past work revealed that the degree distribution of a network alone (i.e., the probability distribution over the number of links that nodes have) is correlated with the minimum number of controls (*1*).

Understanding the control properties of a complex system requires not just knowing how many controls are needed, but also characterizing the functional origin of each control, an explanatory detail not provided by the degree distribution correlation. For example, a biochemical system and a financial system might require the same number of controls, but the structures within the networks that give rise to these controls could be quite different. Ultimately, planning and implementing a control scheme on a network will depend greatly on how these control points are situated in the network.

The formulation of control that we employ, structural controllability, formalizes the idea that, in the absence of a feedback loop (or, more generally, a cycle), a given node can control at most one of its immediate neighbors (*5*). Thus, the structure of the propagation of control influence through the network consists of a backbone of directed paths, called stems, each driven by an independent control (*6*). These paths can then control cycles that are inherently self-regulatory (see supplementary text). However, ultimately it is these stems that dictate the need for controls: There must be one control for each stem in the system (*7*).

An immediate question, then, is how many stems exist in the system. The location of stems is largely dictated by two topological network features: sources, which are nodes with edges only pointing away from them (e.g., node A in Fig. 1), and sinks, which are nodes with edges only pointing toward them (e.g., nodes F and G in Fig. 1). A source, because it does not have edges entering it, can only appear at the origin of a stem and therefore must be directly controlled. Similarly, a sink, lacking edges to influence other nodes, must lie at the end of a stem. The number of stems in a complex system, then, is at least $max(N_s, N_t)$, where N_s and N_t are the number of sources and sinks, respectively. Without lack of generality, we consider here a graph with no disconnected nodes (*8*).

In situations where a path must branch into two or more paths in order to reach all nodes, a dilation occurs: Additional stems must be introduced at these branching points, each one requiring a separate control (see supplementary text). Some of these dilations may arise due to a surplus of sink nodes ($N_t > N_s$). In this case we call the dilations due to surplus sink nodes, $N_e = max(0, N_t - N_s)$, external dilation points (see the branching at node E to F and G in Fig. 1). The remaining stem dilations give rise to a class of controls due to more nuanced network structures, called internal dilation points, N_i (see the branching at node A to nodes B and C in Fig. 1).

Taken together, the minimum number of independent controls (N_c) required for full control of a complex network is, then, the sum of the number of source nodes, external dilation points, and internal dilation points,

$$N_c = N_s + N_e + N_i \quad (1)$$

with N_s, N_e, and N_i not all zero (*4*, *9*). One way to calculate N_c directly is by using a maximum matching algorithm, which, while accurate, is expensive for large networks (see supplementary text).

With this understanding, we can examine the breakdown of the origin of controls in terms of amounts of source nodes, external dilation points, and internal dilation points for different classes of real-world networks, as well as for widely used generative network models (see supplementary text for the complete listing). To make direct comparisons across networks of different size, in the following discussion we normalize by the number of nodes, N, i.e., $(n_s, n_e, n_i) = (N_s/N, N_e/N, N_i/N)$ and $n_c = N_c/N$.

For any network, $n_c^{se} = n_s + n_e$ can be computed directly from the network's degree distribution, namely, the sum of the fraction of nodes with in-degree zero and out-degree zero. This explains why Liu *et al.* found that the degree distribution of a network correlates so strongly with the number of controls (*1*). Our findings show that knowing the full degree distribution is often unnecessary since, on average, the number of con-

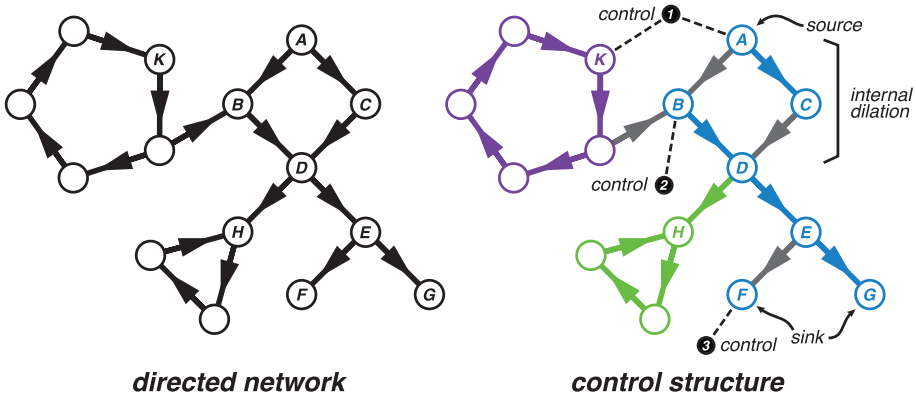

Fig. 1. An example of (left) a simple directed network and (right) one of the possible minimum control structures, constructed of stems (blue) and cycles (purple and green). There is one source (node A) and two sinks (nodes F and G). Three controls are required arising from one source (node A), one external dilation (due to two sink nodes F and G), and one internal dilation (due to the A-B-C-D topology). The dashed lines indicate how control signals enter the network. For control 1, the same signal is sent to nodes A and K. Controls 2 and 3 send different signals to nodes B and F, respectively. Gray arrows indicate edges that are not involved in the control structure of the network. See the supplementary text for additional details regarding the determination of the control structure and its various components.

[1]Engineering Systems and Design, Singapore University of Technology and Design, Singapore. [2]Department of Computer Science, McGill University, Montreal, Quebec, Canada.

*Corresponding author. E-mail: justinruths@sutd.edu.sg

trols is dominated by only two points in the degree distribution: sources and sinks (i.e., nodes with in-degree = 0 or out-degree = 0, respectively).

Indeed, the fraction of nodes that are internal dilation points ($n_i = n_c - n_c^{se}$) is, in many cases, relatively small in both real networks and the random network models that are often used to approximate real-world networks. Across a total of 70 real networks—sampled from ecological, economic, neural, organizational, social, transcriptional, and technological systems (see table S2)—n_i averaged 14.0%. We observed low n_i across random networks as well: 3.0, 3.0, 2.8, and 24.9% in Erdos-Renyi (ER), Barabasi-Albert (BA), local attachment (LA), and duplication-divergence (DD) networks, respectively (*10*–*13*). When n_i is small, as is the case in many networks, the bound given by n_c^{se} is quite tight. Notably, DD networks exhibit a higher fraction of internal dilation points (n_i = 24.9%), but still small enough to meaningfully employ the estimates above.

By simply counting source and sink nodes (a task that is linear in the number of nodes), we obtain a relatively good lower bound on the number of controls. This approach is a marked improvement over the maximum matching algorithm, which is used to obtain the exact number of minimum controls. This algorithm requires computational steps proportional to the number of edges, which can be quadratically greater than the number of nodes (see supplementary text).

Moreover, this estimate performs as well as one based on the full degree distribution, despite requiring much less information. In Fig. 2, we compare the predictive power of using n_s and n_e alone (n_c^{se}, blue) against the number of controls implied by the network's full degree distribution (n_c^{deg}, red). We find that, on average across all the surveyed networks, the additional information from the full degree distribution accounts for only 5.1% improvement in the prediction for real networks and 2.7% (ER), 0.6% (BA), 0.7% (LA), and 7.3% (DD) for synthetic networks (see fig. S1 for further details). This further indicates that additional statistics beyond the degree distribution will be needed to fully capture the number of internal dilations and to reduce these prediction errors.

Although prediction is a powerful use for our framework, we now return to the original question regarding the decomposition of controls in networks. To make an equitable comparison across networks with different numbers of controls, but potentially similar relative composition of controls, we modify Eq. 1 to represent the fractions of controls due to source nodes ($\eta_s = N_s/N_c$), external dilation points ($\eta_e = N_e/N_c$), and internal dilation points ($\eta_i = N_i/N_c$) by normalizing the equation with respect to the number of controls, N_c:

$$\eta_s + \eta_e + \eta_i = 1 \qquad (2)$$

Because N_c can be computed by means of a maximum matching algorithm (see supplementary text), and N_s and N_e are obtained from analysis of node degrees, we can trivially solve for N_i. Our goal is no longer to estimate N_c; hence, defining N_i as a function of N_s, N_e, and N_c is not circular because each of these terms can be directly computed. We obtain the control profile for a complex network, given by the triple (η_s, η_e, η_i). Using these control profiles and their corresponding plots (see fig. S4), we can investigate the extent to which the profiles of networks differ.

We have already established that, of the synthetic networks considered, few have appreciable numbers of internal or external dilations. This is largely due to the way in which these networks are generated. The generative models that yielded networks with few internal dilations had one of two key features. BA and LA networks grow by new node attachment: At each time step, a new node is added that has no inbound neighbors. Preferential attachment further does not favor creating links to these new sources, yielding an enrichment in sources. ER, by contrast, creates sources and sinks with equal probability, making it difficult for generated networks to have substantial numbers of external dilations.

By definition, a dilation requires an expansion point in the network—a region where a smaller number of nodes link into a larger number of nodes. Preferential attachment is biased against expansion, favoring linking into smaller populations of high-degree nodes. ER also has no built-in bias toward expansion points. DD, however, does, by virtue of creating new nodes through copy events (*14*). Overall, this suggests that the expected values of a control profile may be anticipated and understood by appealing to the formation mechanism that generated it rather than particular high-level network properties that the mechanism induces.

Real networks have control profiles that are vastly different from the synthetic networks considered (see Fig. 3). This is related to the observation above—that existing generation methods are biased toward source-based controls. How-

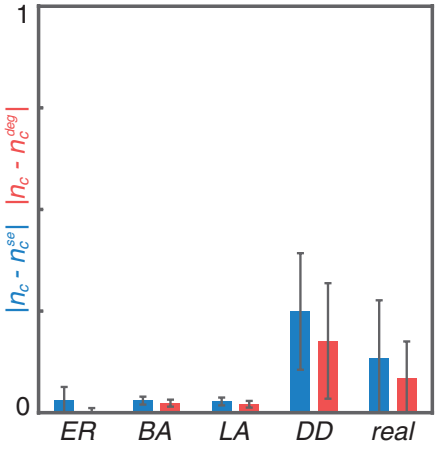

Fig. 2. Source and sink nodes dominate the correlation between degree distribution and the number of required controls. The error in the approximation of the fraction of required controls is only slightly improved by incorporating the nonzero terms of the degree distribution ($n_c^{deg} = N_c^{deg}/N$ is the fraction of required controls after a degree-preserving shuffle; $n_c^{se} = n_s + n_e$ is the fraction of source and sink nodes in the network). The mean improvement in approximation error for synthetic networks—Erdos-Renyi (ER), Barabasi-Albert (BA), local attachment (LA), and duplication-divergence (DD)—and real networks is indicated by the difference in bar heights. Synthetic networks were generated from a comprehensive set of parameters with network sizes, *N*, ranging from 100 to 50,000; average degree, *L*/*N*, ranging from 2 to 58; and for DD networks, a probability to retain copied edges from 0.1 to 0.9 (see supplementary text). The error bars represent one standard deviation from the mean approximation error.

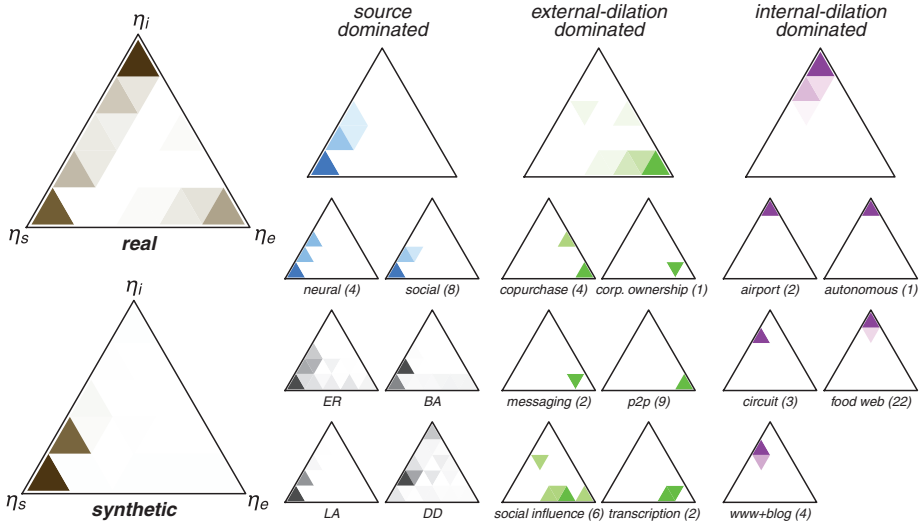

Fig. 3. Real and synthetic networks have substantially different control profiles. The coloring of breakout subfigures indicates the clustering observed in various types of real networks. Deeper shades of the heatmap indicate a greater density of networks with control profiles located in that region. Networks with $N_s = N_t = N_i = 0$ are omitted from this figure (*9*). The aggregated heatmaps are normalized to avoid biases induced by over- and underrepresented types of networks (see supplementary text for details). Numbers in parentheses indicate numbers of networks present in each plot.

ever, more generally, these methods lack the ability to specify a target control profile at all. Thus, in much the same way as many network generation methods have parameters to set specific degree distributions or clustering, future work on controllability in complex networks will require network models in which the control profile can be tuned to match those observed in the real world.

Real networks also have control profiles that are different from the profiles of their randomized counterparts. Figure S3 shows the impact of several randomization schemes, in particular, highlighting the loss or gain of internal dilations indicated visually by a vertical shift in the heatmap density. This suggests that many real networks have an internal dilation signature that distinguishes them from other randomized instantiations.

Although the control profiles of real networks are diverse, they also show a strong tendency to cluster around the three components of the control profile itself, suggesting that real networks broadly fall into three distinct classes: external-dilation dominated, source dominated, and internal-dilation dominated (see Fig. 3). Because these clusters do not correspond to known groupings of networks, we can test the conjecture that similar network types cluster together. These control profile clusters are statistically significant according to two separate tests for such consistency (see table S1 and fig. S2).

Although the class of external-dilation–dominated networks comprises a diverse set of systems, the control profiles of these networks consistently reflect a surplus of sinks, indicating that the systems cannot be fully controlled in a top-down manner (from sources alone). Instead, a control scheme that uses only sources will yield correlated behavior among nodes that are downstream from a common source. Such synchronized behavior may be an objective of the system. For example, in corporate-ownership, leadership, and trust hierarchies, decisions or beliefs at the sources (the owners and leaders) will drive correlated behavior, functional differentiation, and beliefs in owned organizations, followers, and advice-seekers (*15*, *16*). Genes involved in transcriptional systems exhibit such high degrees of correlated expression that these correlations form the basis for cancer diagnosis and staging (*17*–*19*). Similarly, in copurchase networks, many products (accessories) may derive meaning, and therefore shopper relevance, from a smaller set of core products (the items that need to be accessorized). As a result, in each case above, to achieve full controllability, additional controls must be added to nonsource nodes.

Source-dominated networks, unlike the external-dilation–dominated class, have no more sinks than controls. Where an external-dilation–dominated control profile indicated a top-down organization, intended to drive correlated behavior through the system, a source-dominated control profile may suggest the opposite—a tendency toward allowing relatively uncorrelated behavior. This makes distributed processing possible, which is characteristic of the systems that fall into this class: biological neural and social networks. In both, the systems are structured to enable independent computations and interaction at a massive scale (*20*, *21*).

Internal-dilation–dominated networks include food networks, electrical circuits, airport interconnectivity, intranets, and the Internet's autonomous systems. These share a fundamental feature in common: They are all, more or less, closed systems. Reinforcing this idea is that many of these systems obey conservation laws, i.e., Kirchhoff's law for electrical circuits and biomass conservation within an ecosystem. Those that do not have a formal conservation law are still characterized by the circulation and recirculation of a resource (e.g., information and perspectives in the blogosphere and population movement within transportation systems) that drive the evolution of the system's state. Consistent with the notion of a closed system and conservation laws, internal-dilation–dominated networks represent systems that can be intended to function relatively independently of external stimulation.

More generally, external-dilation– and internal-dilation–dominated networks both require many controls to be attached to nonsource nodes in order to provide full controllability. When sources correspond to inputs to the system, we might interpret dilations to be the signature of a network that is not meant to be fully controlled, in that it is not designed to visit every possible system state (e.g., the conservation laws in internal-dilation–dominated networks impose constraints such that only a portion of the full state space can be explored). Indeed, in the case of transcriptional networks, electronic systems, and the Internet, certain states are pathological to or are simply unexplored by a system under natural conditions (*22*). A tantalizing direction for future work is to consider the extent to which internal dilations themselves reveal characteristics of forbidden regions of state space.

Nevertheless, the extent to which the control properties of networks are determined by source nodes can give insight into whether it is actually practical to control the entire system. Sources in a network can correspond to elements that lie on the boundary of the system—variables to which we have direct access. For example, in the case of biochemical pathways in human cells, target receptor proteins responsible for transducing extracellular stimuli into intracellular signals act as source nodes in the cellular signaling network (*23*, *24*). Because these nodes are readily accessible and influence the protein interactions within the cell, a large percentage of drugs used today target these receptor proteins, rather than intracellular proteins directly, to effect change within the cell (*25*). Thus, networks whose control profiles are dominated by sources may have a much more feasible actuation scheme.

Finally, despite surveying a wide array of complex networks, our analysis yields few networks with profiles that contain nontrivial contributions of all three components. This suggests that many complex systems may share in common a general principle that makes such control profiles unfavorable.

Understanding the causal origin of a network's minimal control points can yield both direct and comparative insights into the system and its control properties. Certainly, the scale and organic nature of connectivity present in many complex systems suggest that strategies for controlling them will be nontrivial; thus, such fundamental insights may be crucial to such endeavors.

Here, we have identified the major structures that induce the need for controls in a complex network in order to guarantee controllability. This led to the discovery that for many networks, we can approximate the number of controls simply by the zero-degree points of the degree distribution. Subsequently, we defined the control profile, the decomposition of a complex network into the structural elements that induce the need for specific controls—sources, external dilations, and internal dilations. We find that control profiles highlight a profound and systemic difference between the control structures of random network models and real networks. Furthermore, the control profiles of real networks fall into three clusters that correspond to different aspects of high-level structure and function. Thus, the control profile is a network statistic that may prove useful in better understanding and approaching the control of complex networks.

References and Notes

1. Y.-Y. Liu, J.-J. Slotine, A.-L. Barabási, *Nature* **473**, 167–173 (2011).
2. M. Pósfai, Y.-Y. Liu, J.-J. Slotine, A.-L. Barabási, *Sci. Rep.* **3**, 1067 (2013).
3. T. Jia *et al.*, *Nat. Commun.* **4**, 2002 (2013).
4. In this work, we discuss the minimum number of independent controls (denoted N_c). In some previous literature, this number was called the minimum number of driver nodes (denoted N_D) (*1*).
5. C.-T. Lin, *IEEE Trans. Automat. Contr.* **AC-19**, 201–208 (1974).
6. The structure capturing the propagation of control, composed of stems, cycles, and buds, is called cacti. Each cactus within the cacti contains only one stem and any number of cycles and buds (see supplementary text).
7. C. Commault, J.-M. Dion, J. W. Van der Woude, *Kybernetika* **38**, 503–520 (2002).
8. An immediate extension can be made to accommodate disconnected nodes as stems of unit length, acting as both a source and sink.
9. In the exceptional case where $N_s = N_e = N_i = 0$, at least one control must be present, so $N_c = 1$. Formally we could revise Eq. 1 to $N_c = max(1, N_s + N_e + N_i)$. See supplementary text for more discussion.
10. P. Erdös, A. Renyi, *Publicationes Mathematicae* **6**, 290–297 (1959).
11. A.-L. Barabási, R. Albert, *Science* **286**, 509–512 (1999).
12. M. O. Jackson, B. W. Rogers, *Am. Econ. Rev.* **97**, 890–915 (2007).
13. I. Ispolatov, P. L. Krapivsky, A. Yuryev, *Phys. Rev. E Stat. Nonlin. Soft Matter Phys.* **71**, 061911 (2005).
14. Edge orientation is a matter of convention; see supplementary text for discussion on the sensitivity of our results to edge reversals.
15. S. Vitali, J. B. Glattfelder, S. Battiston, *PLOS ONE* **6**, e25995 (2011).
16. N. E. Friedkin, *A Structural Theory of Social Influence* (Cambridge Univ. Press, Cambridge, 2006).
17. N. Bhardwaj, K.-K. Yan, M. B. Gerstein, *Proc. Natl. Acad. Sci. U.S.A.* **107**, 6841–6846 (2010).
18. H. Yu, M. Gerstein, *Proc. Natl. Acad. Sci. U.S.A.* **103**, 14724–14731 (2006).
19. L. J. van 't Veer *et al.*, *Nature* **415**, 530–536 (2002).
20. E. Bullmore, O. Sporns, *Nat. Rev. Neurosci.* **10**, 186–198 (2009).
21. M. Girvan, M. E. J. Newman, *Proc. Natl. Acad. Sci. U.S.A.* **99**, 7821–7826 (2002).
22. F.-J. Müller, A. Schuppert, *Nature* **478**, E4 (2011).

23. W. K. Kroeze, D. J. Sheffler, B. L. Roth, *J. Cell Sci.* **116**, 4867–4869 (2003).
24. J. S. Gutkind, *Sci. STKE* **2000**, re1 (2000).
25. M. J. Marinissen, J. S. Gutkind, *Trends Pharmacol. Sci.* **22**, 368–376 (2001).

Acknowledgments: We thank the anonymous reviewers for their thoughtful and insightful critiques, which substantively improved this manuscript. Supported by the Singapore University of Technology and Design–Massachusetts Institute of Technology International Design Center (IDG31300103) and by Natural Sciences and Engineering Research Council (Discovery Grant 125517855).

Supplementary Materials
www.sciencemag.org/content/343/6177/1373/suppl/DC1
Materials and Methods
Figs. S1 to S4
Tables S1 and S2
References (*26*–*70*)

18 June 2013; accepted 31 January 2014
10.1126/science.1242063

Fossilized Nuclei and Chromosomes Reveal 180 Million Years of Genomic Stasis in Royal Ferns

Benjamin Bomfleur,[1]* Stephen McLoughlin,[1]* Vivi Vajda[2]

Rapidly permineralized fossils can provide exceptional insights into the evolution of life over geological time. Here, we present an exquisitely preserved, calcified stem of a royal fern (Osmundaceae) from Early Jurassic lahar deposits of Sweden in which authigenic mineral precipitation from hydrothermal brines occurred so rapidly that it preserved cytoplasm, cytosol granules, nuclei, and even chromosomes in various stages of cell division. Morphometric parameters of interphase nuclei match those of extant Osmundaceae, indicating that the genome size of these reputed "living fossils" has remained unchanged over at least 180 million years—a paramount example of evolutionary stasis.

Royal ferns (Osmundaceae) are a basal group of leptosporangiate ferns that have undergone little morphological and anatomical change since Mesozoic times (*1*–*6*). Well-preserved fossil plants from 220-million-year-old rocks already exhibit the distinctive architecture of the extant interrupted fern (*Osmunda claytoniana*) (*2*), and many permineralized osmundaceous rhizomes from the Mesozoic are practically indistinguishable from those of modern genera (*3*–*5*) or species (*6*). Furthermore, with the exception of one natural polyploid hybrid (*7*), all extant Osmundaceae have an invariant and unusually low chromosome count (*7*, *8*), suggesting that the genome structure of these ferns may have remained unchanged over long periods of geologic time (*8*). To date, evidence for evolutionary conservatism in fern genomes has been exclusively based on studies of extant plants (*9*, *10*). Here, we present direct paleontological evidence for long-term genomic stasis in this family in the form of a calcified osmundaceous rhizome from the Lower Jurassic of Sweden with pristinely preserved cellular contents, including nuclei and chromosomes.

The specimen was collected from mafic volcaniclastic rocks [informally named the "Djupadal formation" (*11*)] at Korsaröd near Höör, Scania, Sweden [fig. S1 of (*12*)]. Palynological analysis indicates an Early Jurassic (Pliensbachian) age for these deposits (*11*) (fig. S2), which agrees with radiometric dates obtained from nearby volcanic necks (*13*) from which the basaltic debris originated. The fern rhizome was permineralized in vivo by calcite from hydrothermal brines (*11*, *14*) that per-

[1]Department of Palaeobiology, Swedish Museum of Natural History, Post Office Box 50007, SE-104 05 Stockholm, Sweden. [2]Department of Geology, Lund University, Sölvegatan 12, SE-223 62 Lund, Sweden.
*Corresponding author. E-mail: benjamin.bomfleur@nrm.se (B.B.); steve.mcloughlin@nrm.se (S.M.)

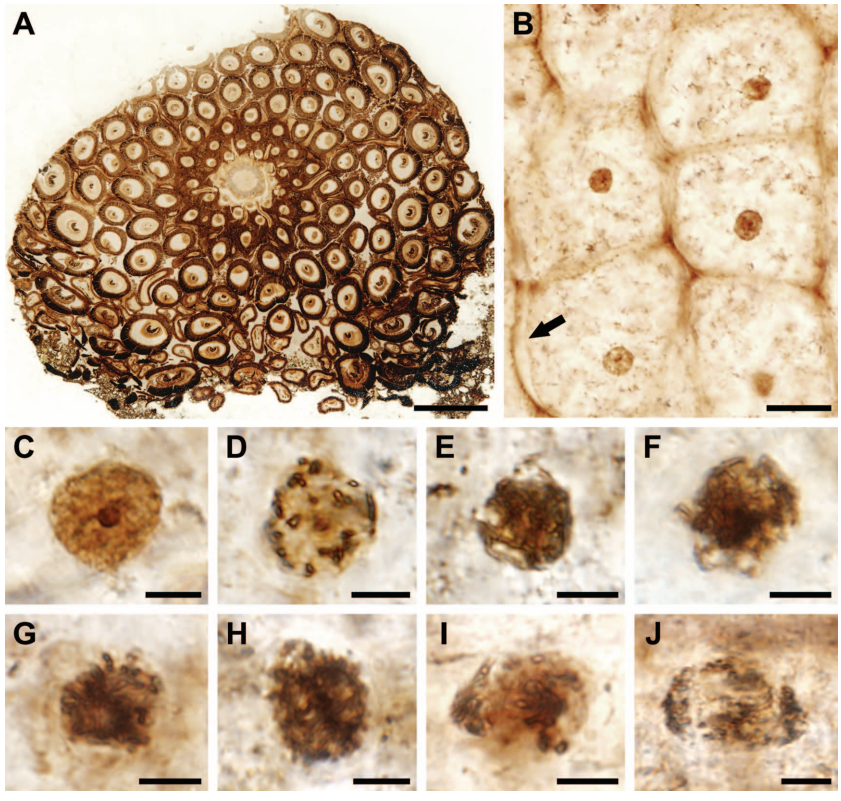

Fig. 1. Cytological features preserved in the apical region of the Korsaröd fern fossil. (**A**) transverse section through the rhizome; (**B**) detail of radial longitudinal section showing typical pith-parenchyma cells with preserved cell membranes (arrow), cytoplasm and cytosol particles, and interphase nuclei with prominent nucleoli; (**C**) interphase nucleus with nucleolus and intact nuclear membrane; (**D**) early prophase nucleus with condensing chromatin and disintegrating nucleolus and nuclear membrane; (**E** and **F**) late prophase cells with coiled chromosomes and with nucleolus and nuclear membrane completely disintegrated; (**G** and **H**) prometaphase cells showing chromosomes aligning at the equator of the nucleus; (**I** and **J**) possible anaphase cells showing chromosomes attenuated toward opposite poles. (A), (C to E), (G), and (I) are from NRM S069656. (B), (F), (H), and (J) are from NRM S069658. Scale bars: (A) 500 μm; (B) 20 μm; (C to J) 5 μm.